is the local eustatic mean relative SLR in year T, in meters [L]; SLR_g is the global mean SLR determined to be 0.0017 m/yr. from observations from 1900 to 1992, [L/T]; SLR_l represents a local mean SLR determined to be -0.00027 m/yr. from observations from 1900 to 1992 for the Galveston Bay [L/T]; $\dot{s}_b$ represents the local bedrock subsidence rate, which is 0.00241 m/yr. in HGR; $\dot{s}_s$ denotes the local secondary consolidation rate of the uncemented Quaternary and semi-cemented Tertiary strata due to geo-historical overburden pressure, which was estimated to be 0.00267 m/yr. in section 3.4 in HGR; bg, global mean SLR acceleration, is 0.0, 8.71×10^{-5}, 2.71×10^{-5} and 1.56×10^{-4} m/yr.^{2} for the lowest, intermediate low, intermediate high, and highest scenarios, respectively (Parris, A., P. Bromirski, V. Burkett, D. Cayan, M. Culver, J. Hall, R. Horton, K. Knuuti, R. Moss, J. Obeysekera, A. Sallenger 2012),(Flick E. R, Knuuti, K., and Gill 2013; NRC 1987; USACE 2013); and $s_{p(T)}$ is the subsidence from primary consolidation due to groundwater withdrawal at year T in meters [L]. From section 3.4, $s_{p(T)}$ is considered to be zero for projection since its rate is zero under HGSD's groundwater level management. The relative sea level rise projection results at Galevston Pier 21 in Galveston Bay is given in Fig. 8. The annual mean relative sea level in Galveston Bay was projected to rise to 0.66, 0.97, 1.67 and 2.48 m in 2100 for the lowest, intermediate low, intermediate high, and highest scenarios, respectively. Compared to the annual mean sea level of -0.04m, the relative sea level was projected to rise 0.70, 1.01, 1.71 and 2.52 m in the 21st century for the lowest, intermediate low, intermediate high, and highest scenarios, respectively. In the projected relative sea level rise values in the 21st century, LS accounts for 72%, 50%, 30% and 20% for the lowest, intermediate low, intermediate high, and highest scenarios, respectively.

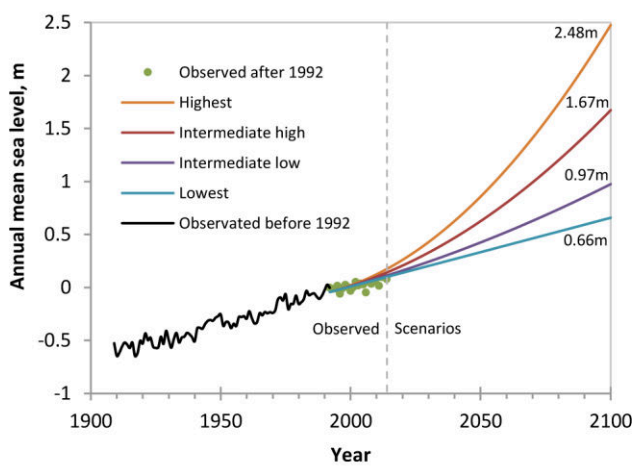

Fig. 8. Relative sea level rise projection at Galveston Pier 21 in Galveston Bay

CONCLUSION

The local relative sea level rise in Galveston Bay consists of global and local mean sea level rise due to global warming, local bedrock subsidence primarily due to tectonic plate motion, primary consolidation subsidence due to groundwater withdrawal from uncemented or semi-cemented aquifer systems, and secondary consolidation subsidence due to geo-historical overburden pressure of the aquifer systems. The projection of a local sea level rise includes projection of all the five components. Global sea level rise acceleration is assumed to be same everywhere in the world. The global and local mean sea level rises are 1.70 and -0.27 mm/yr., respectively. The bedrock subsidence was estimated to be 2.41 mm/yr. based on GPS measurements. The primary consolidation subsidence at Galveston Pier 21 was considered to zero because groundwater level has been managed to be stable in trend since 2000. The local secondary consolidation subsidence was estimated to be 2.67 mm/yr. with time in this paper. The annual mean relative sea level in Galveston Bay was projected to rise to 0.66, 0.97, 1.67 and 2.48 m in 2100 for the lowest, intermediate low, intermediate high, and highest scenarios, respectively. Compared to the annual mean sea level of -0.04m in 2000, the relative sea level was projected to rise 0.70, 1.01, 1.71 and 2.52 m in the 21st century for the lowest, intermediate low, intermediate high, and highest scenarios, respectively. In the projected relative sea level rise values in the 21st century, LS accounts for 72%, 50%, 30% and 20% for the lowest, intermediate low, intermediate high, and highest scenarios, respectively.

ACKNOWLEDGEMENT

This research is supported by the National Science Foundation (NSF) Grant #1832065 entitled as “Identification of urban flood impacts caused by land subsidence and sea level rise in the Houston-Galveston region”.

REFERENCES

Ablain, M., A. Cazenave. 2009. “A New Assessment of the Error Budget of Global Mean Sea Level Rate Estimated by Satellite Altimetry over 1993-2008.” *Ocean Science* 5(2): 193–201.

Alex Wilson. 2017. “Lessons from Hurricane Harvey.”

Allison, I., R. B. Alley, H. A. Fricker, R. H. Thomas, R. C. Warner. 2009. “Ice Sheet Mass Balance and Sea Level.” *Antarct. Sci.* 21: 413.

Arctic Monitoring and Assessment Programme, Oslo, Norway. 2011. “Snow, Water, Ice and Permafrost in the Arctic (SWIPA): Climate Change and the Cryosphere.” http://www.amap.no/documents/download/968.

Baker, E.T. 1979. “Stratagraphic and Hydrogeologic Framework of Part of the Texas Coastal Plain.” *Texas Department of Water Resources* (July): 1–18.

Church, J. A. and N.J. White. 2011. “Sea-Level Rise from the Late 19th to the Early 21st Century.” *Surveys in Geophysics*.

Cuffaro, M., E. Carminati, and C. Doglioni. 2006. “Horizontal versus Vertical Plate Motions.” *eEarth Discussions* 1(2): 63–80. http://www.electronic-earth-discuss.net/1/63/2006/.

Flick E. R, Knuuti, K., and Gill, S.K. 2013. “Matching Mean Sea Level Rise Projections to Local Elevation Datums.” *J. Waterway, Port, Coastal, Ocean Eng.*

Gerald W. Bawden, Michaela R. Johnson, Mark C. Kasmarek, Justin Brandt, and and Clifton S. Middleton. 2012. “Investigation of Land Subsidence in the Houston-Galveston Region of Texas By Using the Global Positioning System and Interferometric Synthetic Aperture Radar , 1993 – 2000.” : 1993–2000.

Gill, Stephen, Neil Weston, and Dru Smith. 2015. *NOAA Guidance Document for Determination of Vertical Land Motion at Water Level Stations Using GPS Technology*.

IPCC. 2014. *Climate Change 2014: Synthesis Report*.

Kasmarek, M.C., J.K. Ramage, and M.R. Johnson. 2016. *Water-Level Altitudes 2016 and Water-Level Changes in the Chicot, Evangeline, and Jasper Aquifers and Compaction 1973–2015 in the Chicot and Evangeline Aquifers, Houston–Galveston Region, Texas*. USGS.

Kasmarek, Mark C. 2013. *Hydrogeology and Simulation of Groundwater Flow and Land-*

Surface Subsidence in the Northern Part of the Gulf Coast Aquifer System, Texas, 1891–2009.

Kennedy J.J., P.W. Thorne, T.C. Peterson, R.A. Ruedy, P.A. Stott, D.E. Parker, S.A. Good, and and K.M. Willett H.A. Titchner. 2010. “How Do We Know the World Has Warmed? [In State of the Climate in 2009].” *Bull. Amer. Meteor. Soc.* 91(6): S26–27.

Lindquist, E. 2009. *Adaptation to Climate Change in the Houston-Galveston Area: Perceptions and Prospects*. http://bush.tamu.edu/research/capstones/mpsa/projects/2009/AdaptionToClimateChange.pdf.

McAllister, T. 2013. *Developing Guidelines and Standards for Disaster Resilience of the Built Environment: A Research Needs Assessment*.

Melillo, J. M., T. C. Richmond, and G. W. Yohe. 2014. *Climate Change Impacts in the United Statess: The Third National Climate Assessment.*

Meyer, W.R., and J.E. Carr. 1979. “A DIGITAL MODEL FOR SIMULATION OF GROUND-WATER HYDROLOGY IN THE HOUSTON AREA, TEXAS.” *Texas Dapartment of Water Resources* (August).

NCEI. 2018. *U.S. Billion-Dollar Weather and Climate Disasters*. https://www.ncdc.noaa.gov/billions/.

NHC. 2017. *Tropical Cyclone Report: Hurricane Harvey*. https://www.nhc.noaa.gov/data/tcr/AL092017_Harvey.pdf.

Nicholls, Robert J., and Anny Cazenave. 2010. “Sea-Level Rise and Its Impact on Coastal Zones.” *Science* 328(5985): 1517–20.

NRC. 1987. *Responding to Changes in Sea Level: Engineering Implications*. National R. Washington, D.C.: National Academy Press.

NRC. 1991. *Mitigating Losses from Land Subsidence in the United States*. National R. Washington, D.C.: National Academy Press.

NWC. 2009. *Flood Damages Suffered in the United States during Water Year 2007*.

NWC. 2015. “Hydrologic Information Center - Flood Loss Data.” *NOAA’s National Weather Service*. http://www.nws.noaa.gov/hic/.

NWS. 2013. *Flood Damages Suffered in the United States during Water Year 2007*. http://www.nws.noaa.gov/hic/summaries/WY2013.pdf.

NWS. 2014. *Flood Damages Suffered in the United States during Water Year 2007. National Oceanic and Atmospheric Administration*. http://www.nws.noaa.gov/hic/summaries/WY2014.pdf.

Parfomak, P.W. 2005. *Vulnerability of Concentrated Critical Infrastructure: Background and Policy Options*.

Parris, A., P. Bromirski, V. Burkett, D. Cayan, M. Culver, J. Hall, R. Horton, K. Knuuti, R. Moss, J. Obeysekera, A. Sallenger, and J. Weiss. 2012. *Global Sea Level Rise Scenarios for the United States National Climate Assessment*. Silver Spring, MD. http://scenarios.globalchange.gov/sites/default/files/NOAA_SLR_r3_0.pdf.

Schwartz, H. G. 2010. “Climate Change. National Academy of Engineering.” *The Bridge* 40(3): 5–14. https://www.nae.edu/Publications/Bridge/24514/24525.aspx.

Schweikert, A., Chinowsky, P., Espinet, X., & Tarbert, M. 2014. “Climate Change and Infrastructure Impacts: Comparing the Impact on Roads in Ten Countries through 2100.” *Procedia Engineering* 78: 306–16.

Sellards, E H, W. S. Adkins, and F.B. Plummer. 1932. “The Geology of Texas: Volume 1 Stratigraphy.” *University of Texas Bulletin* (3232): 1007.

Tebaldi, Claudia, Benjamin H. Strauss, and Chris E. Zervas. 2012. "Modelling Sea Level Rise Impacts on Storm Surges along US Coasts." *Environmental Research Letters* 7(1).
USACE. 2013. *INCORPORATING SEA LEVEL CHANGE IN CIVIL WORKS PROGRAMS*.
Walsh, J., D. Wuebbles, K. Hayhoe, J. Kossin, K. Kunkel, G. Stephens, P. Thorne, R. Vose, M. Wehner, J. Willis, D. Anderson, S. Doney, R. Feely, P. Hennon, V. Kharin, T. Knutson, F. Landerer, T. Lenton, J. Kennedy, and R. Somerville. 2014. "Ch. 2: Our Changing Climate." In *Climate Change Impacts in the United States: The Third National Climate Assessment*, U.S. Global Change Research Program, 19–67. doi:10.7930/J0KW5CXT.
Wilbanks, J. J. 1974. "Educational Reductionism." *Educational Theory* 24(1): 73–78. doi: 10.1111/j.1741-5446.1974.tb00625.x.
Zervas, C, S Gill, and W Sweet. 2013. "Estimating Vertical Land Motion from Long-Term Tide Gauge Records." *NOAA Tech. Rep. NOS CO-OPS 065*. http://scholar.google.com/scholar?hl=en&btnG=Search&q=intitle:Estimating+Vertical+Land+Motion+from+Long-Term+Tide+Gauge+Records#2.

A Decision Support Tool for Constructing Rainfall Intensity-Duration-Frequency Relations in the Context of Climate Change

Van-Thanh-Van Nguyen, M.ASCE[1]; and Truong-Huy Nguyen[2]

[1]Dept. of Civil Engineering and Applied Mechanics, McGill Univ., 817 Sherbrooke St. West, Montreal, QC H3A 2K6, Canada. E-mail: van.tv.nguyen@mcgill.ca
[2]Dept. of Civil Engineering and Applied Mechanics, McGill Univ., 817 Sherbrooke St. West, Montreal, QC H3A 2K6, Canada. E-mail: huy.nguyen5@mail.mcgill.ca

ABSTRACT

Intensity-duration-frequency (IDF) relations are essential for estimating extreme rainfalls for design of various hydraulic structures. The construction of these relations represents however a challenging and tedious task since it involves the uncertainty analysis of different probability models and the frequency analyses of a large amount of extreme rainfall data for different durations at a given site or over many different locations. This paper proposes hence a decision-support tool, herein referred to as SMExRain, that can readily be used to identify in an objective and systematic manner the most suitable distribution(s) for accurate and robust estimation of design rainfalls. In addition, in the context of a changing climate, the proposed tool include a statistical downscaling procedure for describing the linkage between climate predictors given by global climate models and the daily and sub-daily extreme rainfalls at a given site. Results of an illustrative application using climate simulations from different global climate models and extreme rainfall data for Ontario region, Canada, has demonstrated the accuracy and practical usefulness of the SMExRain for establishing reliable IDF relations at a given site for present and future climates.

INTRODUCTION

Rainfall frequency analyses are commonly used for the design of various urban hydraulic structures, such as dams, culverts, and storm sewers. Results of these analyses are often summarized by “intensity-duration-frequency” (IDF) relations for a given site or they are presented in the form of “rainfall frequency atlas”, which provides rainfall accumulation depths for various durations and return periods over the region of interest (see, e.g., WMO 2009; Environment Canada 2014). In current engineering practices, the IDF relations are derived based on statistical frequency analyses of annual maximum rainfall series (AMS) data where available rainfall records of adequate lengths could be used to estimate the parameters of a selected probability distribution (WMO 2009; CSA 2012).

In general, selection of a suitable distribution to representing AMS is the most difficult and time-consuming task since there are many recommended probability models available in the literature as well as in the national design guidelines from different countries (Stedinger et al. 1993; Hosking and Wallis 1997; WMO 2009; CSA 2012; ARR 2016). Recently, a systematic approach has been proposed by Nguyen et al. (2017) to identify the most appropriate probability distributions among several candidate models for providing the most accurate and most robust extreme rainfall estimates. This systematic approach has been shown to be more efficient and more robust than the traditional model selection method since it was based on two main steps: (i) a detailed evaluation of both descriptive and predictive abilities of a probability model as well as its uncertainty (rather than only the descriptive ability as in most previous studies); and (ii) a systematic comparison of the accuracy and robustness of all candidate models based an extensive set of graphical and numerical performance criteria.

Descriptive ability relates to the goodness of fit of the theoretical probability model to the empirical frequency distribution given by the observed extreme rainfall data while the predictive ability is concerned with the accuracy and robustness of the extreme rainfall quantile estimates given by the selected model using the rainfall data in the validation period (that are different from those data used in the calibration of the selected model). This predictive ability assessment, however, is a highly time-consuming task since it requires the generation of a large number of random rainfall samples (for instance, by bootstrap method) for different rainfall durations (from several minutes to hours or days) for establishing the IDF relations for a given site, or for constructing the regional rainfall frequency maps using the data from many different locations over a given region. Consequently, based on the advanced computing capability of existing computer systems it is necessary to develop a decision-support tool that could facilitate the application of the proposed systematic model selection approach in an efficient manner in order to be able to identify automatically and objectively the best probability models for a large number of datasets

In addition, the derivation of IDF relations at a location of interest in the context of climate change is one of the most challenged tasks in current engineering practices (Willems et al. 2012; Simonovic et al. 2016). This IDF derivation requires an advanced rainfall modelling approach that could establish an accurate linkage between climate projections from global or regional climate models and daily and sub-daily extreme rainfall processes at a local site of interest. In the present study, the spatio-temporal statistical downscaling (STSD) method will be used for estimating extreme rainfall IDF relations at a given site in consideration of climate change (Nguyen and Nguyen, 2018). The proposed approach uses the daily downscaled CMIP5 climate projections available at the regional scale (approximately 25 x 25 km) that has been produced by NASA based on the outputs from the 21 global climate models (GCMs) using the bias-correction spatial disaggregation technique (Thrasher et al., 2012). The NASA daily extreme rainfalls were first spatially downscaled to a local site of interest. Then the scale-invariance probability weighted moments-based Generalized Extreme Values (GEV/PWM) model was used to downscale the daily extreme rainfalls to sub-daily amounts at the same location (Nguyen and Nguyen, 2018).

In view of the above issues, the main objective of the present study is to propose a decision-support tool (hereafter referred to as SMExRain – Statistical Modelling of Extreme Rainfalls) that can be used for the construction of IDF relations at a given location or for a large number of sites in the context of current and future climates. The structure of the SMExRain and the procedure for identifying the best distribution is described in Section 2. An illustrative application of this decision-support tool using daily and sub-daily AMS data for Ontario region is presented in Section 3. Results of this numerical application have indicated the accuracy and high efficiency of the proposed SMExRain tool.

THE DECISION SUPPORT TOOL - SMEXRAIN

The main components of the SMExRain

SMExRain has been coded in Matlab environment and equipped with a user-friendly interface. It can independently run without any requirement of a Matlab version. However, it requires the installation of the free-of-charge Matlab Compiler Runtime (MCR) v9.1

corresponding to the Matlab R2016b version (Mathworks 2016). Note that using an incompatible MCR may cause the program to be malfunction. Figure 1 shows the different main components of the SMExRain tool.

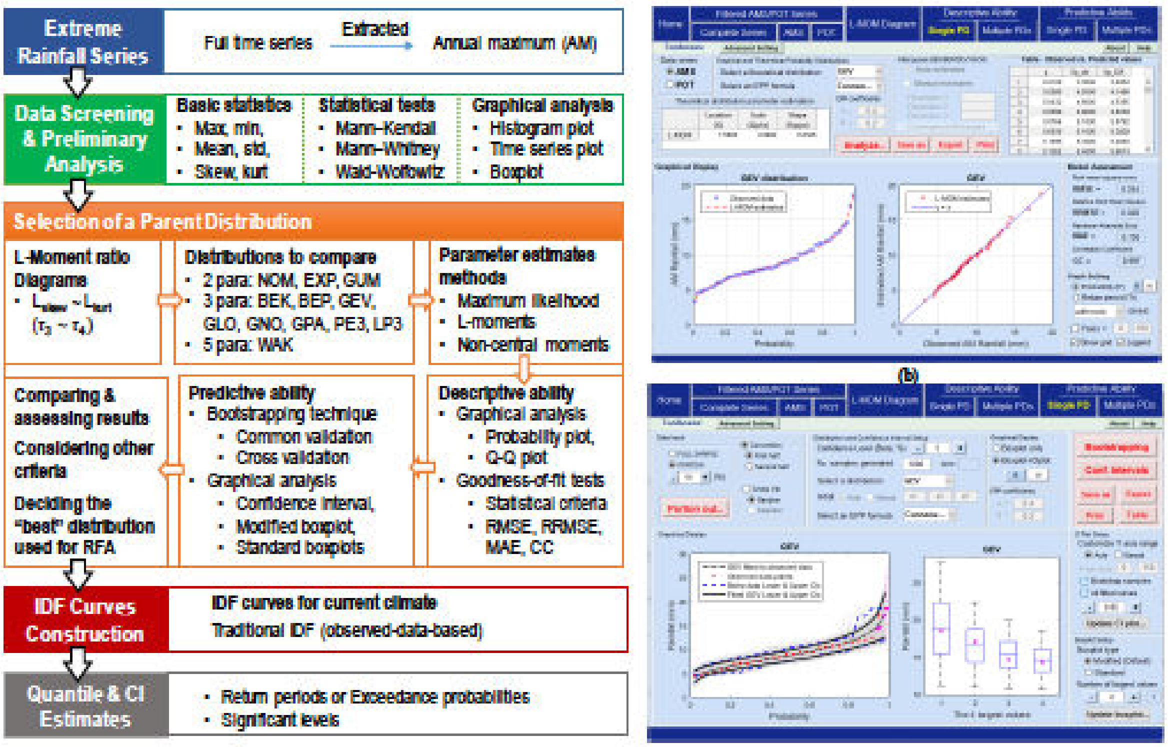

(a) (c)

Figure 1. The main components of SMExRain

The first component is the extraction of the AMS series for different durations from the complete rainfall record. The second component is dealing with the data screening and preliminary statistical analysis step. SMExRain provides several common statistical data analysis procedures based on computed numerical indices and graphical display format, including the histogram plots for empirical probability function analysis, the time series plot for trend analysis, and the boxplot for outlier detection. Furthermore, three statistical tests were included for testing the independence and stationarity of the input data series: the Mann-Whitney test for homogeneity and stationarity (jumps), the Mann–Kendall test for trend detection, and the Wald-Wolfowitz test for independence and stationarity (Rao and Hamed 2000; WMO 2009). The third component involves the selection of a best-fit probability distribution based on various numerical and graphical criteria, including some common tools such as the popular L-moment ratio diagram, different statistical GOF tests, and various graphical displays. In addition, SMExRain provides necessary tools for evaluating the predictive ability of a model. For convenience, SMExRain allows users to perform the assessment and comparison of up to twelve probability distributions simultaneously rather than to evaluate a single distribution at a time. The fourth component is the construction of IDF relations for the current and future climates, and the final component is the computation of extreme rainfalls for different selected return periods and their associated confidence intervals.

Probability distributions and parameter estimation procedures

SMExRain includes several common probability distributions that have been selected based on their popularity in hydrologic frequency analyses: Beta-K (BEK), Beta-P (BEP), Generalized Extreme Value (GEV), Generalized Normal (GNO), Generalized Logistic (GLO), Generalized Pareto (GPA), Gumbel (GUM), Log-Pearson Type III (LP3), Pearson Type III (PE3), and Wakeby (WAK) distributions. Other special cases of these distributions, such as exponential (EXP) and normal (NOM) were also included in the software. Regarding the estimation of the distribution parameters, the method of L-moments is used for all distributions (Hosking and Wallis 1997) except for the BEK and BEP models that are estimated by the method of maximum likelihood (Mielke and Johnson, 1974). GEV parameters are estimated by both the L-moments (denotes as GEV) and non-central moments (denotes as GEV*) methods (Nguyen et al. 2017).

Furthermore, it is noted that the parameter (or quantile) estimates of some distributions, such as BEK, BEP, GNO, PE3, LP3, GEV*, are in implicit forms and they require iterative solving methods. Numerical methods are thus utilized to obtain approximate solutions. SMExRain relies on the accuracy of the f-solve function supported by MATLAB with the three well-known and powerful algorithms, including the trust-region dogleg, the trust-region-reflective, and the Levenberg-Marquardt to achieve feasible solutions (Mathworks, 2016). In addition, to enhance the accuracy and to speed up the quantile estimates processes of the GNO/NOM and PE3/LP3 distributions, SMExRain was equipped with the normal inverse and incomplete gamma inverse functions (Mathworks, 2016).

Goodness-of-fit (GOF) tests for assessing the descriptive ability of a distribution

To visually assess the GOF of a fitted distribution to an observed rainfall dataset, the SMExRain provides probability plots and quantile-quantile (Q-Q) plots (see Figure 1b). Many commonly-used empirical plotting position (EPP) formulas available in the literature are included in this software (Cunnane, 1978; Nguyen et al., 1989; Inna and Nguyen, 1989). In addition, it also provides a general user-customized EPP formula. In addition to the visual assessment, SMExRain includes also four popular numerical indices to provide a more accurate evaluation of the best fit of a distribution; namely, the root mean square error (RMSE), the relative root mean square error (RRMSE), the maximum absolute error (MAE), and the correlation coefficient (CC) (see Nguyen et al. 2017). Furthermore, to facilitate the identification of the probability models with the best descriptive ability, a convenient ranking scheme has been developed to judge the overall GOF of each distribution. Rankings are assigned to each distribution according to the computed values of these numerical indices. For instance, a distribution with the lowest RMSE, RRMSE, MAE and highest CC would be given the rank of 1. In the case of a tie, average ranks are assigned to those tied distributions.

Assessment of the predictive ability of a distribution using bootstrap method

The bootstrap method repeatedly draws, with replacement, n observations from the available data set of size N (N>n) (Efron and Tibshirani, 1994). First, a portion of "n" data points from the original sample of size N (n < N) is selected. In SMExRain, two options are provided: common validation and cross validation. In the former option, users can select the first or second half of a given sample to do bootstrapping. In the latter option, a portion of the sample of size n can be extracted with the starting point selected randomly. Then the bootstrap samples (hundreds to thousands) are generated based on these "n" selected values. The default value is 1000 samples for reliable results and efficient computation costs. Each candidate distribution is then fitted to the generated bootstrap samples and is extrapolated to estimate the right-tail quantiles corresponding to the k largest (k=4 by default) observed rainfall amounts in the full data set (N values). The variability in the estimation of these extrapolated quantiles is presented in the form of modified boxplots by default. However, users can also easily switch to the standard boxplots (Helsel and Hirsch 2002). Large box widths or long whiskers imply high uncertainty in the estimation of these k largest rainfall values. If the observed values fall outside the box, then the distribution fitted to the bootstrap samples has overestimated or underestimated the true values and this distribution is therefore not recommended since it does not provide accurate rainfall estimates. Note that SMExRain allows user to compare the predictive ability of up to twelve models simultaneously using the same generated samples to ensure a fair comparison.

Construction of IDF relations for current and future climates

In SMExRain, the IDF relations are provided in both tabular and graphical forms for the computed rainfall intensities (or depths) for different durations (usually from five minutes to one day) and for different return periods of interests (commonly from two to a hundred years). Depending upon the empirical mathematical model selected for representing the IDF relations, the coefficients (parameters) of this model are computed using the least-square technique. In general, the mathematical form of the empirical model is chosen such that it can facilitate the interpolation of rainfall intensities for a given observed duration or interpolated (unobserved) duration. SMExRain supports many popular regression equations in both real-space (with two or three coefficients) and log-space (with polynomial up to order 6) based on some available practical guidelines (WMO 2009; ARR 2016). A further detail related to the use of different regression-based methods in hydrologic frequency analysis can be found in Pandey and Nguyen (1999).

As indicated above, in the present study the spatio-temporal statistical downscaling (STSD) method will be used for estimating extreme rainfall IDF relations at a given site in consideration of climate change (Nguyen and Nguyen, 2018). Two approaches are employed for transferring the NASA extreme rainfalls at the regional 25-km scale, $\hat{X}$, to a given local site, X_i. The first method uses a scaling factor to correct the mean (MEAN) of the regional dataset and the at-site dataset. In details, the regional values are adjusted by a scaling factor as defined by Eqn. (1). Whereas, the second method utilizes a bias correction function to correct the residuals of the entire empirical cumulative distribution function (ECDF) or empirical quantiles matching between two datasets. In details, the regional values are adjusted by a bias correction function as defined by Eqn. (2). The coefficients of the bias correction function to estimate to the residuals associated with the regional values $\hat{X}$ could be obtained fitting a regression model (i.e. a second-degree polynomial) as described in Eqn. (3) (Nguyen et al. 2007; Nguyen and Nguyen 2008; Willems et al. 2012)

$$X_i(F) = \eta_i \cdot \hat{X}(F) \; ; \tag{1}$$

$$X_i(F) = \hat{X}(F) + e(F) \; ; \tag{2}$$

$$e(F) = c_o + c_1 \cdot \hat{X}(F) + c_2 \cdot [\hat{X}(F)]^2 + \varepsilon \tag{3}$$

where $X_i(F)$ is the adjusted daily extreme rainfall series at the local site of interest i; $\hat{X}(F)$ is the daily regional extreme rainfall series at the grid containing that site; F is the cumulative probability of interest; $\eta_i = \mu_i / \hat{\mu}$ is the scaling factor at site i; μ_i and $\hat{\mu}$ are the expected means (i.e. estimated based on sample means) of the daily extreme rainfall series at the local site of interest i and at the grid containing that site; $e(F)$ is the residual associated with $\hat{X}(F)$; $c_o, c_1, and\, c_2$ are the coefficients of the bias correction function and ε is the resulting error term.

After obtaining the daily extreme rainfall series at the location of interest, the second step is to derive the statistical properties of sub-daily extreme rainfall series at the same site. To do this, the scale-invariance probability weighted moment-based Generalized Extreme Values (GEV/PWM) model was used. The GEV distribution has been widely used for representing the probability distribution of extreme rainfalls and for constructing the rainfall IDF relations (Schaefer 1990; WMO 2009). It has been also recommended in the national guidelines of Australia and of many other European countries, for example, Austria, Germany, Italy, and Spain (Ball et al. 2016; Salinas et al. 2014). The scale-invariance (or scaling) concept has increasingly become a new methodology in the analysis and modeling of various hydrological processes across a wide range of temporal scales (Gupta and Waymire 1990; Burlando and Rosso 1996; Sposito 1998; Hubert 2001; Lovejoy and Schertzer 2012). The GEV/PWM has been recently proposed by Nguyen et al. (2018) and has been shown to perform superior than the other existing scale-invariance models.

NUMERICAL APPLICATION

Study sites and data

The climate simulation outputs from 21 global climate models (GCMs) conducted under the Coupled Model Inter-comparison Project Phase 5 (CMIP5) and the observed IDF data from a network of 84 raingages located in Ontario, Canada, were used for this study. In this paper, for illustrative purposes, only results from the application of the SMExRain for Ontario were presented based on a total of 252 rainfall datasets for three rainfall durations (5 minutes, 1 hour, and 24 hours).

The climate simulation outputs have been statistically downscaled by NASA (i.e., NASA Earth Exchange) from the global scales (a few degrees or 10^2 km) to the regional scale (approximately 25 km × 25 km) for two different Representative Concentration Pathways scenarios (i.e. RCP 4.5 and 8.5) based on the bias-correction spatial disaggregation approach. Each of the precipitation projections contains data for the periods from 1950 through 2005 ("Retrospective Run") and from 2006 to 2100 ("Prospective Run"). Note that only the data from 1961 to 1990 were used for the calibration processes while those from 1991 to 2005 were used for the validation purposes. The prospective precipitation projections were used to construct future IDF relations.

Descriptive ability assessment results

The Q-Q plots of all 252 AMS shows that all distributions closely described the left-tail and central parts. The right-tail parts, however, are less well described and there are no obvious trends. These values can be accurately estimated, over-estimated, or under-estimated by any of the 11 candidates. For purposes of illustration, Figure 2 shows the results for 1-hour AMS from the longest rainfall record available at Toronto Int. Airport station. From the visual standpoint, all distributions seem to perform well in this case, except the BEK and GPA distributions. However, the significance of the differences between the remaining models is difficult to judge